Fabrication of M-CNT/TiO$_2$ (M=Cr, Mn and Fe) composites and the effect of transition metals on their photocatalytic activities

Ming-Liang Chen[a], Feng-Jun Zhang[a,b], Kan Zhang[a], Ze-Da Meng[a] and Won-Chun Oh[a*]

[a]*Department of Advanced Materials & Science Engineering, Hanseo University, Seosan-si, Chungnam-do 356-706, Korea*
[b]*Anhui Key Laboratory of Advanced Building Materials, Anhui University of Architecture, Anhui Hefei 230022, P. R. China*

3-Chloroperbenzoic acid has been used to oxidise a multi-walled carbon nanotube (MWCNT) to obtain more functional groups. Chromium trioxide, manganese oxide and ferric nitrate were used to pretreat the oxidised MWCNT and together with titanium *n*-butoxide as titanium precursor to prepare M-CNT/TiO$_2$ composites. FTIR spectroscopy was used to determine the functional groups on the MWCNT and the characterisation of M-CNT/TiO$_2$ composites was by scanning electron microscopy, transmission electron microscopy, X-ray diffraction and energy dispersive X-ray analysis. Methylene blue was used to determine the photocatalytic activities of the M-CNT/TiO$_2$ composites under visible light.

TiO$_2$ is a low cost, radiation stable, non-toxic white pigment with broad applications in optical devices.[1,2] It is also a well-known, high band-gap semiconducting photosensitive material for photo-anodes[3] and photo-catalysts.[4] In fact, TiO$_2$ is noted for its high photocatalytic activity for the degradation of pollutant chemicals.[5] Anatase has higher photocatalytic activity and has been studied more than the other two forms of TiO$_2$,[6] but its wide band gap (3.2 eV) and high electron–hole recombination rate limit the use of TiO$_2$,[7] and it does not act with solar light effectively. Therefore, current research has sought to improve the photocatalytic properties of TiO$_2$ by doping with metals and oxides.[8–10] The presence of metal ion dopants in the TiO$_2$ crystalline lattice significantly influences photoreactivity by changing charge carrier recombination rates and interfacial electron-transfer rates by shifting the band gap of the catalysts into the visible region.[11] A dopant ion may act as an electron trap or hole trap. This would prolong the lifetime of the generated charge carriers, resulting in an enhancement in photocatalytic activity.

Carbon nanotubes (CNTs) have attracted considerable attention since their discovery[12] due to their special structure and extraordinary mechanical and unique electronic properties.[13] Recently, researchers have shown that CNTs as support materials can increase the photocatalytic activity of TiO$_2$.[14,15] Also, CNTs can be used as promising materials for environmental cleaning. The surface area of CNTs is much less than that of activated carbon. Therefore, adsorption is not the only factor for enhancing the photocatalytic activity of TiO$_2$ by CNTs. In our previous work,[16,17] we indicated that MWCNT/TiO$_2$ composites have more photocatalytic activity than pristine TiO$_2$ under irradiation by UV light and the MWCNT could use its photoabsorption character to absorb a photo-induced electron (e$^-$), which could then be introduced into the conduction band of the TiO$_2$ particles and react with O$_2$, which can trigger formation of the very reactive superoxide radical ion (O$_2^-$ $^{\bullet}$).

In the present study, M-CNT/TiO$_2$ composites (M=Cr, Mn and Fe) have been prepared by a sol-gel method. The composites have been characterised by different techniques and their photocatalytic activities were tested by degradation of methylene blue (MB) under visible light.

Experimental

Reagents
A multi-walled carbon nanotube (MWCNT) was selected as the support material. The MWCNT (95.9 wt%, diameter: ~20 nm, length: ~5 µm) was supplied from Carbon Nano-Material Technology Co., Ltd,

Korea and used without further purification. Titanium *n*-butoxide (TNB, 99%), used to form the TiO$_2$, was purchased from Acros Organics (New Jersey, USA). Chromium trioxide (CrO$_3$), manganese oxide (MnO$_2$) and ferric nitrate [Fe(NO$_3$)$_3$] were purchased from Samchun Pure Chemical Co., Ltd, Korea. For the oxidisation, 3-chloroperbenzoic acid (MCPBA) was purchased from Acros Organics, New Jersey, USA. Benzene (99.5%) and HNO$_3$ were purchased from Samchun Pure Chemical Co., Ltd, Korea. MB was the analytical grade solvent used, and it was purchased from Dukan Pure Chemical Co., Ltd. The structure of MB, molecular formula: C$_{16}$H$_{18}$N$_3$SCl, is shown in Fig. 1.

Surface modification of MWCNTs
For preparing the oxidising agent, MCPBA (1 g) was dissolved in benzene (60 mL), then MWCNT (0.5 g) was added. The mixture was stirred magnetically for 6 h at 343 K. Then the modified MWCNT product was dried at 373 K.

Preparation of M-CNT
CrO$_3$, MnO$_2$ and Fe(NO$_3$)$_3$ were used as transition metal precursors. Firstly, CrO$_3$, MnO$_2$ and Fe(NO$_3$)$_3$ were dissolved in H$_2$O, HNO$_3$ and H$_2$O, respectively, to prepare 0.5 M CrO$_3$, MnO$_2$ and Fe(NO$_3$)$_3$ solutions, then oxidised MWCNT (0.5 g) was put into the 0.5 M CrO$_3$, MnO$_2$ and Fe(NO$_3$)$_3$ solutions (30 mL) under stirring on a hot plate for 6 h at 343 K, respectively, then evaporated at 373 K. After heat treatment at 773 K for 1 h, the M-CNT was obtained.

Preparation of M-CNT/TiO$_2$ composites
TNB (4 mL) was dissolved in benzene (46 mL) with stirring then the M-CNT was added. The mixture was then stirred magnetically for 5 h at 343 K. The mixture was then kept at room temperature until it formed a uniform suspension. To obtain the M-CNT/TiO$_2$ composites, the mixture was thermally treated at 873 K for 1 h with a heating rate of 279 K/min. The resulting samples were named as CCT, MCT and FCT, corresponding to use of CrO$_3$, MnO$_2$ and Fe(NO$_3$)$_3$ as transition metal precursors, respectively.

Characterisation
Synthesised composites were characterised by various techniques. The functional groups formed on the surface of MWCNT were examined using FT-IR spectroscopy in Kbr discs. Discs for the method were prepared by first mixing powdered oxidised MWCNT (1 mg) with KBr (600 mg) in an agate mortar, and then pressing the resulting mixture under a pressure of 450 Pa for 3 minutes. The spectra of the samples were measured between 3000 and 500 cm^{-1} using a FTS 3000MX (Biored Co. USA) spectrophotometer. SEM (JSM-5200,
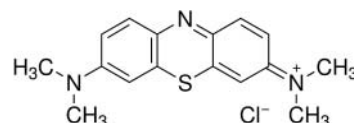
Fig. 1 The structure of MB.

JOEL, Japan) and TEM (JEM-2010, JEOL, Japan) were used to observe the surface state and structure of the M-CNT/TiO$_2$ composites. XRD was used for crystal phase identification and estimation of the anastase-to-rutile ratio. XRD patterns were obtained at room temperature with a Shimata XD-D1 instrument using CuKα radiation. EDX was used to measure the elemental analysis of the M-CNT/TiO$_2$ composites. For determining the photocatalytic activity of M-CNT/TiO$_2$ composites, UV-Vis spectra for the MB solutions obtained from degradation by M-CNT/TiO$_2$ composites dispersion under visible light irradiation were recorded using an Optisen POP spectrometer (Mecasys Co., Korea).

Photocatalytic decomposition
The photocatalytic activities of M-CNT/TiO$_2$ composites were determined by using MB decomposition in aqueous solution under visible light (8W, KLD-08L/P/N, Fawoo Technology). The initial MB concentration was 1.0×10^{-5} mol L^{-1}. The amount of suspended composite was kept at 1 g L^{-1} in 50 mL MB solution. Before turning on the visible lamp, the solution mixed with composite was kept in the dark for at least 2 h, allowing the adsorption–desorption equilibrium to be reached, then the solution was irradiated with visible light. The first sample was taken out at the end of the dark adsorption period (just before the light was turned on), in order to determine the MB concentration in solution, which was hereafter considered as the initial concentration (c_0) after dark adsorption. Samples were then withdrawn regularly from the reactor in the order 30 min, 60 min, 90 min and 120 min, and immediately centrifuged to separate any suspended solid. The clean transparent solution was analysed by using a UV-Vis spectrophotometer (250–600 nm).[18] The spectra (550–750 nm) for each sample were recorded and the absorbance was determined at characteristic wavelength (660 nm) for each MB solution degraded. For comparing the photocatalytic effect, the pristine TiO$_2$ and CNT/TiO$_2$ composite which we prepared in our previous work[16,17] were used as reference samples.

Results and discussion

Surface morphology
FT-IR was conducted on functionalised MWCNT and their corresponding spectra are shown in Fig. 2. After oxidation by MCPBA, the MWCNT have various kinds of functional groups. The bands at 2910 cm^{-1} and 2847 cm^{-1} are assigned to C–H stretching vibrations and the bands at 1695 cm^{-1}, 1303 cm^{-1} and 2847 cm^{-1} to C=O, S=O and C–H stretching vibrations, respectively. The above observations suggest that oxidation was promoted in all treatments, and the functional groups that are formed can increase the active sites on the surface of the MWCNT.[19,20]
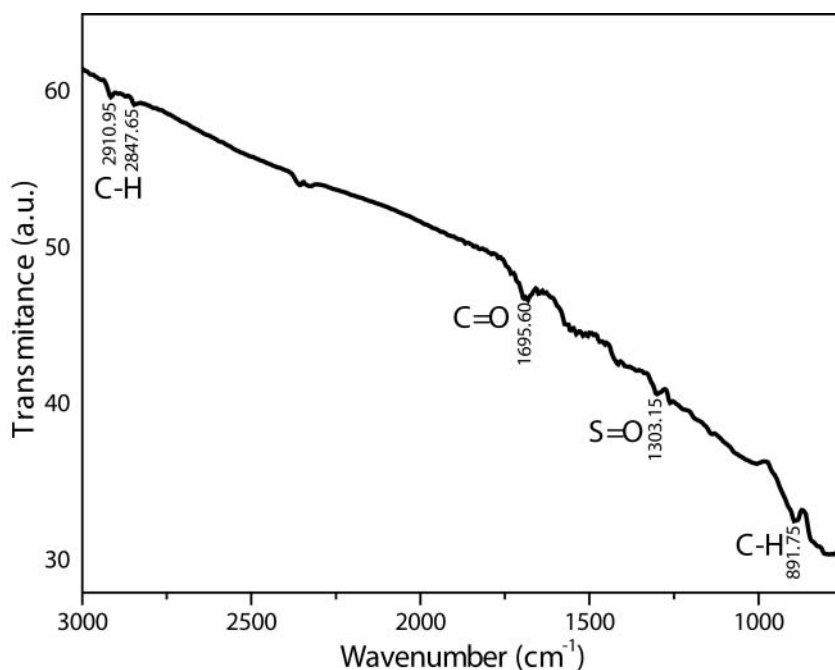
The micro-surface structures and morphology of M-CNT/TiO$_2$ composites were characterised by SEM and TEM. Figure 3 shows the SEM images of M-CNT/TiO$_2$ composites. For sample CCT, there is large agglomeration of Cr$_2$O$_3$ and TiO$_2$ particles together with MWCNT, and some clumpy structure can be observed in Fig. 3(a). For sample MCT, the TiO$_2$ particles and manganese oxide particles mixed with CNT networks and formed a larger block. For sample FCT, the particles of TiO$_2$ were uniformly distributed on the whole CNTs surface. All of the SEM images of M-CNT/TiO$_2$ composites cannot correctly distinguish the structure of metal, TiO$_2$ and CNT, so we used TEM to obtain more detailed observations of the prepared M-CNT/TiO$_2$ composites.

Figure 4 shows the TEM images of M-CNT/TiO$_2$ composites. For the sample CCT, the Cr$_2$O$_3$ and TiO$_2$ particles were homogenously distributed on the surface of MWCNT. These structures would be shown to have excellent photocatalytic activity. For sample MCT, the TiO$_2$ particles were still distributed uniformly on the outside surface of CNT tube and Mn particles were completely attached on the surface of the tube although this caused partial agglomeration. For sample FCT, all the Fe and TiO$_2$ particles are dispersed on the surface of the CNT and have a very narrow sise distribution. As is known, a good dispersion of small particles should provide more reactive sites for the reactants than aggregated particles.

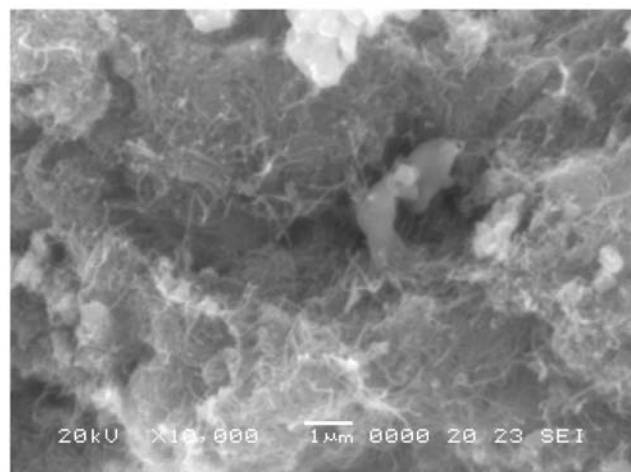*Characterisation of M-CNT/TiO$_2$ composites*
The XRD results for the M-CNT/TiO$_2$ composites are shown in Fig. 5. For all samples, the peaks at 25.3, 37.8, 48.0 and 62.5 are the diffractions of the (101), (004), (200) and (204) planes of anatase, and there are no peaks at 27.4, 36.1, 41.2 and 54.3 belonging to the diffraction peaks of (110), (101), (111) and (211) of rutile, indicating that TiO$_2$ was formed in only one phase, anatase. It is also clearly seen that the sample FCT has a stronger intensity of anatase than other two samples. It could be considered that the sample FCT would have more photocatalytic activity than other samples. In addition, for sample CCT, characteristic peaks are clearly found at 24.5, 33.6, 36.2, 41.4, 50.5, 54.8, 63.6 and 64.5 which belong to chromium oxide (Cr$_2$O$_3$). This indicates that the precursor chromium trioxide (CrO$_3$) has been changed to chromium oxide (Cr$_2$O$_3$); for sample MCT, the peaks attributed to MnTiO$_3$ can be seen on the XRD curve; for sample FCT, the 'Fe+2TiO$_3$' peaks can be found in the XRD curve. The formation of metal oxide can shift the TiO$_2$ absorbtion to the visible light region and increase the photoinduced electrons in the visible light range due to its lower band gap.[21] On the other hand, the characteristic peaks of CNTs could hardly be identified from the XRD patterns of all samples. It was thought that the absence of CNTs aggregated pores
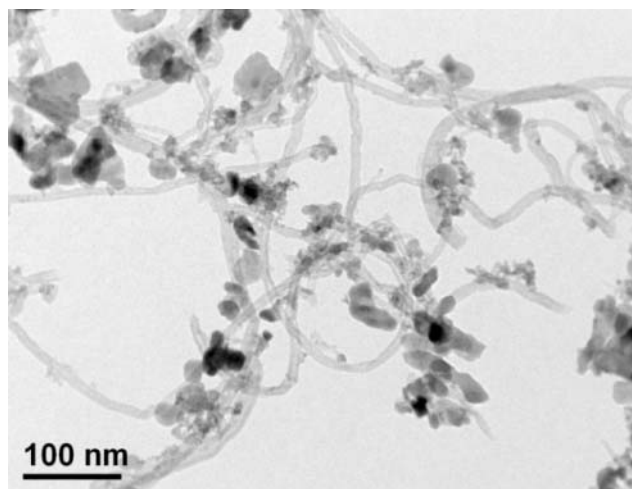

Fig. 2 FT-IR spectra of oxidised MWCNT.
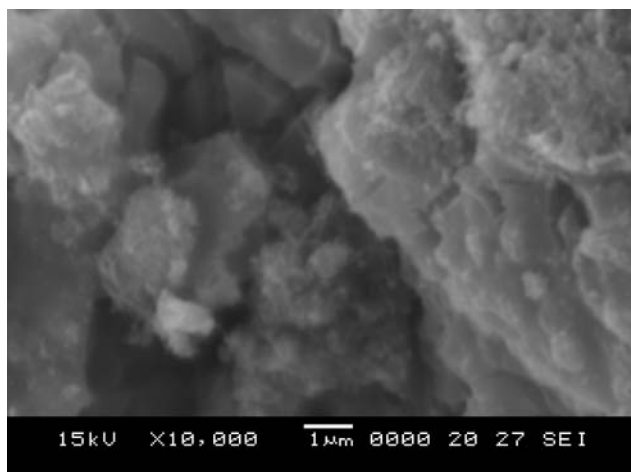
(a)
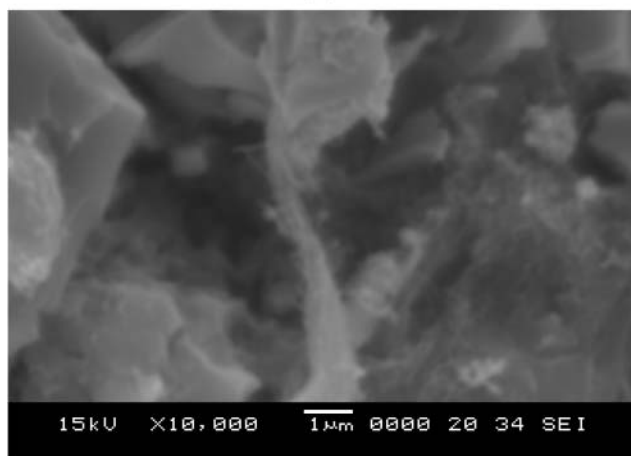
(b)

(c)

Fig. 3 SEM images of metal-CNT/TiO$_2$ composites; (a) CCT, (b) MCT and (c) FCT.
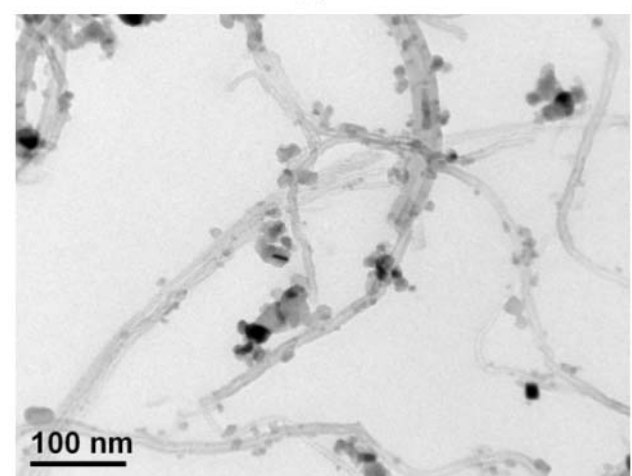

(a)

(b)

(c)

Fig. 4 TEM images of metal-CNT/TiO$_2$ composites; (a) CCT, (b) MCT and (c) FCT.

was supported by the disappearance of CNTs characteristic peaks in the XRD patterns.
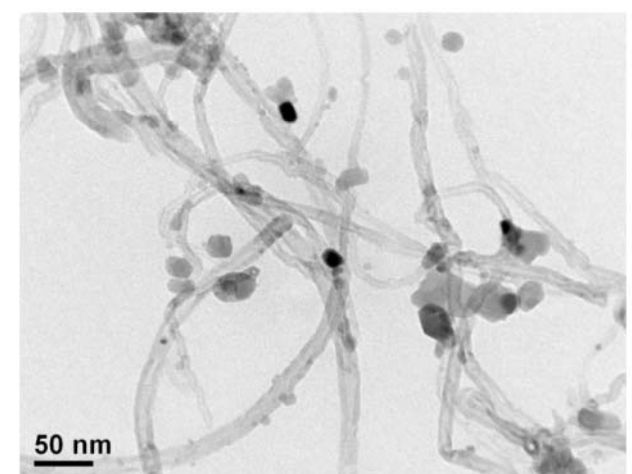
EDX was conducted on several zones of the M-CNT/TiO$_2$ composites. The wt% of main elements found in a representative analysis are listed in Table 1. As observed from Table 1, three kinds of main elements C, O and Ti existed in all samples and Cr, Mn and Fe existed in samples CCT, MCT and FCT, respectively, without any other element impurities.

Photocatalytic degradation of MB solutions

The changes in relative concentration (c/c_0) of MB solutions upon visible light irradiation for the pristine TiO$_2$, CNT/TiO$_2$ composite and M-CNT/TiO$_2$ composites were determined and the results are shown in Fig. 7. The concentration of MB solution was decreased by an increase of irradiation time for all samples. As mentioned above, TiO$_2$ can only show photocatalytic activity under UV light, due to its wide
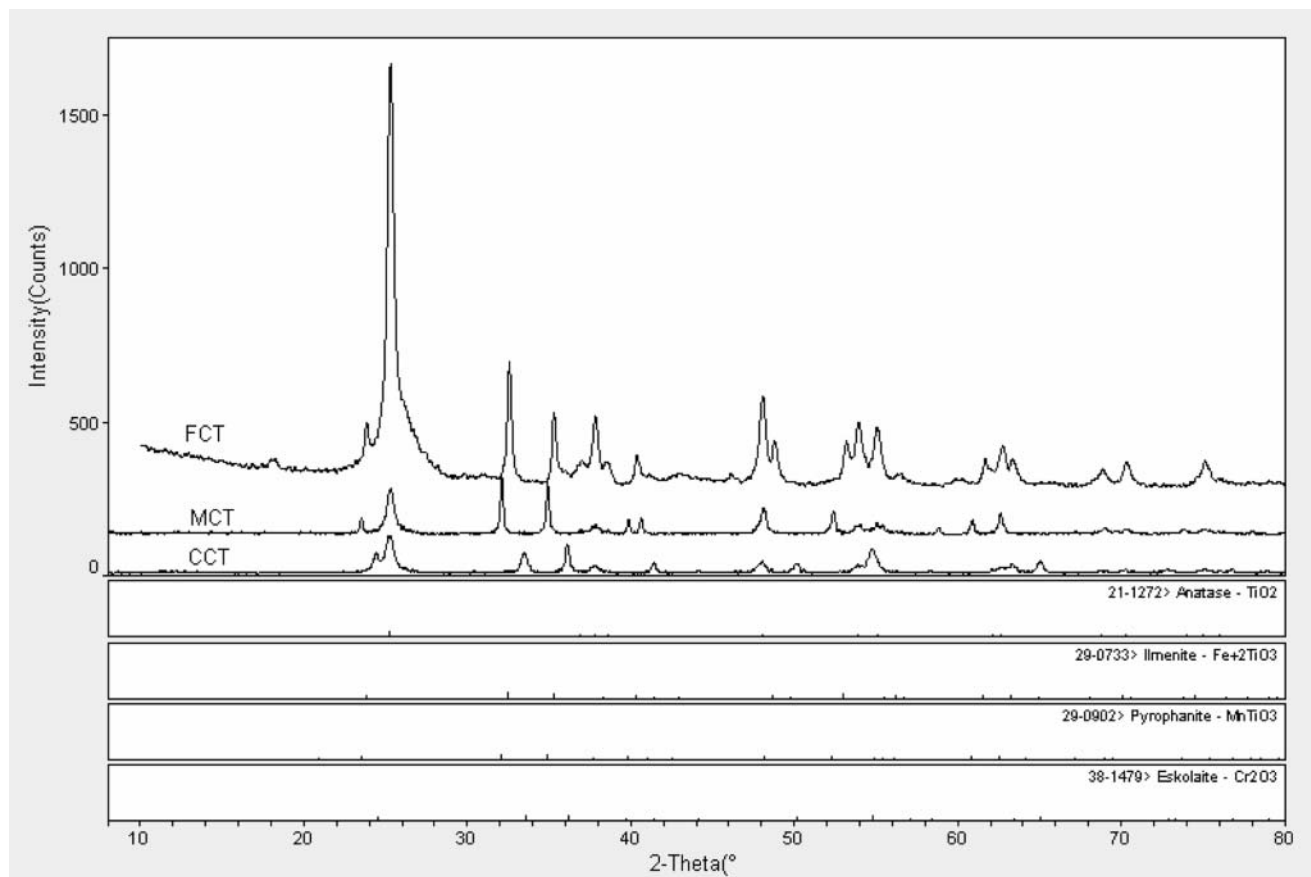
Fig. 5   The XRD patterns of metal-CNT/TiO$_2$ composites which were heat treated at 873 K.

Table 1   EDX elemental microanalysis (wt %) of Cr/CNT/TiO$_2$ composites

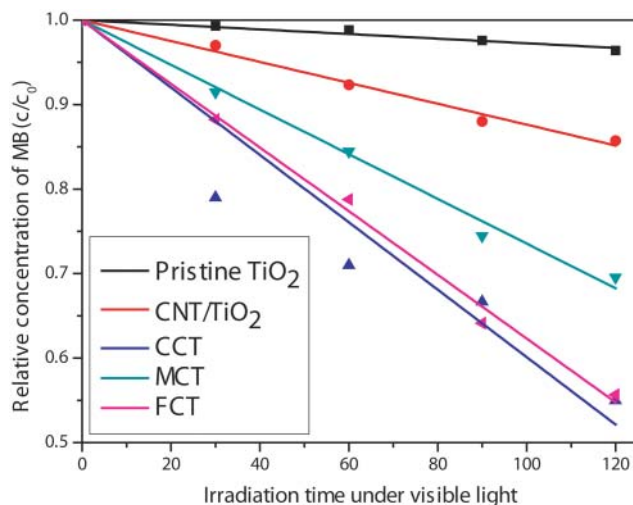| Samples	Elements					
	C	O	Ti	Cr	Mn	Fe
CCT	24.21	39.15	17.77	18.87	–	–
MCT	27.1	40.6	26.4	–	5.9	–
FCT	44.58	19.53	23.71	–	–	12.18

Fig. 6   Comparison of the photodegradation of MB in aqueous solution for pristine TiO$_2$, CNT/TiO$_2$ composite and M-CNT/TiO$_2$ composites; MB: 1.0×10^{-5} mol L^{-1}.

band gap (3.2 eV for anatase), and does not act with solar light effectively. So in the present study, pristine TiO$_2$ shows little photocatalytic activity, only decreasing the MB solution by 3.4% under visible light after 120 min. For the CNT/TiO$_2$ composite, after irradiation for 120 min under visible light, the concentration of MB solution was decreased by 15%, more than pristine TiO$_2$. In our previous work,[16,22,23] it was shown that MWCNT could use its photoabsorption character to absorbed photons from irradiation light, thus increasing the amount of electrons (e$^-$). Therefore, the CNT/TiO$_2$ composite shows more photocatalytic activity than pristine TiO$_2$. M-CNT/TiO$_2$ composites show much more photocatalytic activity than the CNT/TiO$_2$ composite and the concentration of MB solution was decreased by 48%, 32% and 46% for samples CCT, MCT and FCT, respectively. In addition, the apparent kinetic constant (k_{app}) of the pristine TiO$_2$, CNT/TiO$_2$ composite and M-CNT/TiO$_2$ composites shows the same result. Table 3 shows the apparent kinetic constant (k_{app}) of the pristine TiO$_2$, CNT/TiO$_2$ composite and M-CNT/TiO$_2$ composites. The apparent kinetic constant (k_{app}) of the pristine TiO$_2$ and CNT/TiO$_2$ composite is 2.74×10^{-4} min^{-1} and 1.24×10^{-3} min^{-1}. However, the k_{app} of M-CNT/TiO$_2$ composites is much higher than that of pristine TiO$_2$ and CNT/TiO$_2$ composites, which are 3.99×10^{-3} min^{-1}, 2.64×10^{-3} min^{-1} and 3.77×10^{-3} min^{-1}, respectively. Thus it can be seen that the M-CNT/TiO$_2$ composites have higher photocatalytic activities under irradiation of visible light.

According to the TEM images, we can consider that two metal oxides together with the carbon nanotube were observed for sample CCT. The well-crystallised materials have better electron transfer behaviour than the less crystallised materials. In this study, we could observe that the sample CCT has good crystallization from the XRD data. An electron transfer takes place from TiO$_2$ particles to Cr$_2$O$_3$ particles through the carbon nanotube to form an oxidation site at the TiO$_2$ particles and a reduction site at the Cr$_2$O$_3$ particles. Therefore the electron transfer path for sample CCT can be drawn as shown in Fig. 8.[24,25]

However, for samples MCT and FCT, the mechanism of photodegradation for MB solution is different from sample CCT as shown in

Table 2 Apparent kinetic constant (k_{app}) of pristine TiO_2, CNT/TiO_2 composite and metal-CNT/TiO_2 composites for MB degradation

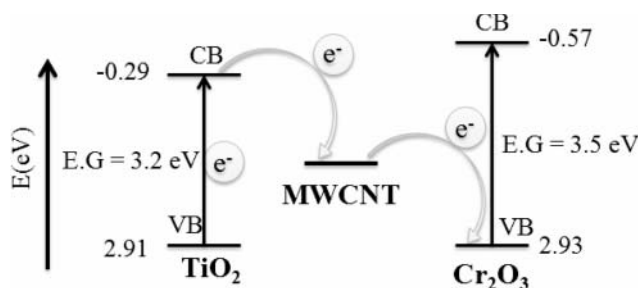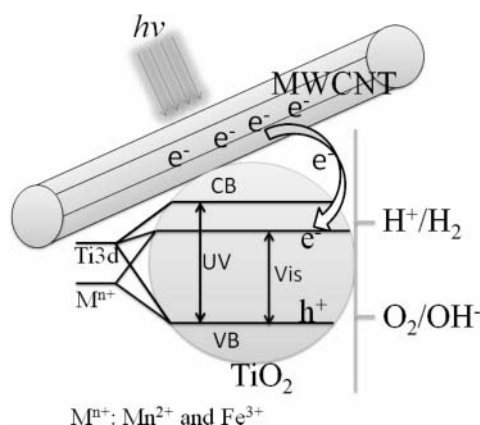| Samples	k_{app} (min^{-1})
Pristine TiO_2	2.74×10^{-4}
CNT/TiO_2 composite	1.24×10^{-3}
CCT	3.99×10^{-3}
MCT	2.64×10^{-3}
FCT	3.77×10^{-3}

Fig. 7 The mechanism of photocatalytic effect of sample CCT for MB solution under visible light.

Fig. 8 The mechanism of M^{n+} in shifting the band-gap of TiO_2 and photocatalytic effect of samples MCT and FCT for MB solution under visible light.

Fig. 9. When transition metal ions are incorporated into the lattice of TiO_2, their level appear between the valence band (VB) and the conduction band (CB) of TiO_2,[26] thus altering the band-gap energy and shifting the absorbance edge to the visible light region.

Moreover, as mentioned above, the MWCNT could use its photoabsorption character to absorb electrons (e$^-$) photo-induced by irradiation and transfer them into the conduction band of the TiO_2 particles, thus increasing their electron density. In this way, the M-CNT/TiO_2 composites showed excellent photocatalytic activities under irradiation by visible light.

Conclusions

M-CNT/TiO_2 composites have been prepared for the transition metals Cr, Mn and Fe, and their photocatalytic activities determined by using MB solution under visible light. From the XRD results, all of samples showed a single phase of anatase for TiO_2, and have Cr_2O_3, $MnTiO_3$ and $Fe+2TiO_3$ structure for samples CCT, MCT and FCT, respectively. As observed from EDX data, three kinds of main elements C, O and Ti existed in all samples and the metal Cr, Mn and Fe were present in samples CCT, MCT and FCT, respectively without any other element impurities. The micro-surface structures and morphology of M-CNT/TiO_2 composites had metal and TiO_2 particles homogenously distributed on the surface of the MWCNT according to TEM images. According to the data of MB degradation, the M-CNT/TiO_2 composites showed excellent photocatalytic activities for MB solutions under irradiation of visible light. For sample CCT, an electron transfer process $TiO_2\rightarrow$carbon nanotube$\rightarrow Cr_2O_3$ occurs. However, for samples MCT and FCT, the transition metal ions incorporated into the lattice of TiO_2, could alter the band-gap energy and shift the absorbance edge to the visible light region. Moreover, the MWCNT could also absorb a photo-induced electron (e$^-$) and transfer it into the conduction band of the TiO_2 particles, thus increasing the electron availability.

References

1 B.E. Yoldas and T.W. O'Keefe, *Appl. Opt.*, 1979, **18**, 3133.
2 M. Lottiaux, C. Boulesteix, G. Nihoul, F. Varnier, F. Flory, R. Galindo and E. Pelletier, *Thin Solid Films*, 1989, **170**, 107.
3 A. Fujishima and K. Honda, *Nature*, 1972, **238**, 37.
4 M.R. Hoffmann, S.T. Martin, W. Choi and D.W. Bahnemann, *Chem. Rev.*, 1995, **95**, 69.
5 S.N. Frank, *J. Am. Chem. Soc.*, 1977, **99**, 4667.
6 M.A. Barakat, H. Schaeffer, G. Hayes and S. Ismat-Shah, *Appl. Catal. B: Environ.*, 2005, **57**, 23.
7 J.C. Colmenares, M.A. Aramendia, A. Marinas, J.M. Marinas and F.J. Urbano, *Appl. Catal. A: Gen.*, 2006, **306**, 120.
8 Y. Zhang, A. Weidenkaff and A. Reller, *Mater. Lett.*, 2002, **54**, 375.
9 M.M. Rahman, K.M. Krishna, T. Soga, T. Jimbo and M. Umeno, *J. Phys. Chem. Solids.*, 1999, **60**, 201.
10 K.M. Krishna, M. Mosaddeq-ur-Rahman, T. Miki, K.M. Krishna, T. Soga, K. Igarashi, S. Tanemura and M. Umeno, *Appl. Surf. Sci.*, 1997, **113/114**, 149.
11 X. Ji-Chuan, S. Yan-Li, J.E. Huang, B. Wang and L. Hu-Lin, *J. Mol. Catal. A: Chem.*, 2004, **219**, 351.
12 S. Iijima, *Nature*, 1991, **354**, 56.
13 T.W. Ebbesen, H.J. Lezee, H. Hiura, J.W. Neentt, H.F. Ghaemi and T. Thio, *Nature*, 1996, **382**, 54.
14 Y. Yu, J.C. Yu, C.Y. Chan, Y.K. Che, J.C. Zhao, L. Ding, W.K. Ge and P.K. Wong, *Appl. Catal. B*, 2005, **61**, 1.
15 Y. Yu, J.C. Yu, C.Y. Chan, Y.K. Che, J.C. Zhao, L. Ding, W.K. Ge and P.K.Wong, *Appl. Catal. A*, 2005, **289**, 186.
16 M.L. Chen and W.C. Oh, *Bull. Korean Chem. Soc.*, 2008, **29**, 159.
17 M.L. Chen, F.J. Zhang and W.C. Oh, *Analyt. Sci. Technol.*, 2008, **21**, 553.
18 M.L. Chen, C.S. Lim and W.C. Oh, *J. Ceram. Process. Res.*, 2007, **8**, 119.
19 W.C. Oh and M.L. Chen, *J. Ceramic Processing Research*, 2007, **8**, 316.
20 F. Aviles, J.V. Cauich-Rodriguez, L. Moo-Tah, A. May-Pat and R. Vargas-Coronado, *Carbon*, 2009, **47**, 2970.
21 O. Giraldo, S. L. Brock, W.S. Willis, M. Marquez and S.L. Suib, *J. Am. Chem. Soc.*, 2000, **122**, 9330.
22 M.L. Chen, F.J. Zhang and W.C. Oh, *J. Korean Ceram. Soc.*, 2008, **45**, 651.
23 M.L. Chen, F.J. Zhang and W.C. Oh, *New Carbon Materials*, 2009, **24**, 159.
24 Y.L. Dong, J.L. Won, S. Jae Sung, H.K. Jung and S.K. Yang, *Comput. Mater. Sci.*, 2004, **30**, 383.
25 Y. Xu and M.A.A. Schoonen, *Am. Mineral.*, 2000, **85**, 543.
26 H. Miyazaki, H. Matsui, T. Nagano, S. Karuppuchamy, S. Ito and M. Yoshihara, *Appl. Surf. Sci.*, 2008, **254**, 7365.